

by

F. W. Smith¹ and H. S. Boyne²

1. Introduction

Figure 1 is a schematic showing the essential characteristics of a snow pillow installation for the SNOTEL system. The snow pillow array is bedded in sand, soil or similar material to provide a firm support. Tubing is connected to the pillow array and extends to a nearby shelter where it connects to a manometer and to a pressure transducer. The pillow array, the tubing, manometer and transducer are all filled with a mixture of methanol and water. The pressure transducer provides an electrical signal which indicates the fluid pressure which is a measure of the amount of snow accumulation on the pillow array. The manometer provides a means to visually check the pressure readings.

A number of difficulties occur in the routine field use of these simple appearing devices. For example, it is found in some installations that during the heat of summer days, the pressure indication may vary by as much as 3.0 inches of water. Variations in manometer readings are also experienced in winter due to solar heating of the SNOTEL shelters. It is important to develop understanding of these temperature effects in assessing the accuracy of SNOTEL readings. The diurnal temperature effect can influence the no-snow zero readings and the wintertime temperature effects on manometer readings can influence the interpretations of the readings.

Air in the connecting tubing has been observed to have some influence on the pillow system behavior. It has been speculated that the size and type of connecting tubing has an influence. It is generally observed in the field that the metal snow pillow measurements of snow water equivalence are higher than measurements taken from a pit density profile or from corrected federal sampler readings.

In an attempt to isolate the causes of these observed difficulties the experiments and analyses described herein were undertaken. The controlled laboratory conditions in these experiments were selected to eliminate the uncontrolled variables present in the field so attention could be concentrated upon the basic behavior of the snow pillow, tubing, manometer system.

2. Pillow Calibration in Test Chambers

The pillow test chamber apparatus is shown in Figure 2. The pillows are bedded in sand. The Watersaver Co. of Denver has constructed the hypalon pressure transmitting bladder and it has been successfully used several times. The presence of the bladder allows the air in the sand under the pillow to remain at atmospheric pressure while uniform air pressures of up to 260 inches of water may be applied to the top of the pillow. This arrangement allows simulation of uniform snow loading conditions.

The test chambers have been used to test a variety of plumbing arrangements on '78 and '79 California pillows as well as SNOTEL pillows. The results are presented in Figures 3 and 4. Figure 3 shows pillow response for 1/4 inch and 1/2 inch copper tubing tested on a 1979 California pillow. Ten of the data points were obtained using the hypalon bladder and the rest without. These tests confirm that the bladder and the plumbing types do not affect pillow performance under laboratory conditions. Tests of this type were also done using 1/4, 3/8 and 1/2 inch diameter polyfic tubing with the same outcome. Figure 4 includes data from experiments with a SNOTEL pillow. Ten of the data points were obtained with a '78 California pillow, 10 with a '79 California pillow and 10 with a SNOTEL pillow. From Figure 4 we conclude that under laboratory conditions, SNOTEL pillows behave about the same as California pillows.

¹Professor, Department of Mechanical Engineering, Colorado State University

²Professor, Department of Earth Resources, Colorado State University

Figures 3 and 4 graphically indicate linear and repeatable behavior. However, the results of linear regression show standard deviations of 0.31 and 0.44 in H_2O which indicates substantial scatter, possibly as much as ± 1.0 in. H_2O . Difficulty with the manometer reading arrangement is thought to be responsible for this level of scatter. The arrangement of the test apparatus was changed and improved to allow reliable reading of the manometer to a precision of about $\pm .031$ in. H_2O . Figure 5 shows the results of repeating the pressure chamber experiment very carefully with a 1979 California pillow. Careful examination of these data reveal the following things. The squares and stars on Figure 5 refer to two different experiments on the same pillow. Clearly, the second experiment very closely repeated the first. Also, the increasing and decreasing pressure data points repeated quite closely. The difference between these readings is about 0.6 in H_2O . It is interesting that the increasing pressure readings were low while the decreasing pressure readings were high indicating a systematic hysteresis in the pillow behavior. Checks were made to insure that this behavior was not being caused by a time lag in the manometer readings.

Perhaps the most interesting observation to be made about Figure 5 is that the data do not plot on a straight line. There is a very slight concave downward curvature, but it is of such size that the peak deviation of a data point from a least square fit straight line through the origin is about 2.0 in. H_2O .

3. Skin Stiffness Experiments

A direct measurement of the pillow skin stiffness was desired because the pillow modeling and nonuniform loading experiments described later in this report indicated that the stiffness of the skin could be important in some cases.

The direct measurement of skin stiffness was conducted as follows: 1.) The pillow was assumed to deflect only vertically so that any volume change can be represented by $\Delta V = A d$ where d is the skin deflection and A is the pillow area. The chamber-pillow-manometer system was brought to steady state at pillow fluid pressure P_1 and applied air pressure P_1' . 2.) The applied pressure was increased to $P_2' = P_1' + 1.0$ in. H_2O , producing a new pillow pressure P_2 . 3.) A volume of fluid was then drained from the pillow until the original pillow pressure P_1 was reached again while holding the applied pressure P_2' constant. The decrease in fluid volume forces the skin to take up the increased applied pressure P_2' as it deforms inward.

The experiment produces two loading states for the pillow. One where the pillow manometer reads P_1 and a second state where the pillow manometer still reads P_1 , but the applied pressure is 1.0 in. H_2O greater than in the first case. The skin stiffness can then be directly calculated by

$$k = \frac{1.0}{d} \text{ in. } H_2O/\text{in. skin deflection}$$

where d is determined from the experimental results using the expression

$$d = \frac{\Delta V}{A_P}$$

In this expression ΔV is the volume of fluid drained out in step 3.

The average value of k for the '78 California pillow was 9.5 in. H_2O /in. deflection and the average value for the '79 California pillow was 15.2 in. H_2O /in. deflection. These results are used in section 5 of this paper.

4. Nonuniform Loading Experiments

A 1978 California pillow was loaded with a variety of uniform and nonuniform distributions using a large number of red firebricks. These tests were performed to learn more about pillow response to nonuniform loading and the importance of the skin stiffness. Specifically, it was felt that a snow pillow would average its load differences to some extent, but that the skin stiffness would limit the averaging process.

Common red firebricks (2'' x 3'' x 7-1/2'') were used. Pillow response to over 1600 pounds of bricks distributed across the upper surface of the pillow in several geometries was measured. Pyramid, wedge and rectangular shaped stacks were built up on the entire pillow surface, half the pillow surface or diagonally across the pillow surface in the various tests. The type of tests conducted are identified in Table I and assigned a code letter. The results of each test are given in Table II including the weight of bricks in each test. Using the brick weights given, the average pressure due to brick weight acting over the total pillow area is given for each test and identified as H_{calc} . It is recognized that the pillow edges do not transmit pressure to the pillow fluid so a pressure is also given in the last column of Table II based on a corrected pillow area taken to be 2592 in.² which was chosen to be 10 per cent less than the actual pillow area. The 10% correction was chosen on the basis that this correction provides agreement between the pressure change measured and H_{calc} for the case where 5 flat layers of bricks were applied.

The results in Table II show that the pillow does not average the applied nonuniform pressure. All of the data support the conclusion that the pillow senses a weighted average.

The pyramid and wedge data are plotted in Figure 6 as a function of the load gradient. The load gradient is approximately the brick pile slope. For example, in the 16 brick high pyramid test, the load on the pillow changes from zero psi at the outer edge of the pillow to approximately 2.73 psi in the center yielding a load gradient of 1.09 psi/foot. All of the points plotted in Figure 6 represent total pillow loads of 1617 lbs. The pillow's increased sensitivity to central loads is demonstrated. For the steepest pyramid loading case the pillows overweigh by as much as 30 per cent. For the wedge loading case, most of the load is applied near the edge of the pillow which produces an underweighing error of up to 20 per cent for the cases tested. The half block also underweighs as do the diagonal wedge and diagonal block loading cases.

The five type 'C' tests with uniform layers of brick indicate agreement to within less than 0.2 in. H_2O difference between the manometer readings corrected to in. H_2O and the calculated average pressure based upon a pillow effective area. Recall that the effective area is taken to be 90 per cent of the actual pillow area because the area near the pillow edges responds very weakly to applied pressure.

5. Pillow Performance Models

It is desirable to model a snow pillow system including thermal expansion effects in order to assess diurnal and seasonal head changes due to temperature changes of various parts of the system. For modeling purposes, the system is separated into N pillows, N ground tubes and one manometer. There are two quantities to be calculated 1.) The manometer head, and 2.) The pillow deflection. These heads are defined relative to the base of an idealized pillow as shown in Figure 1. The pillow is idealized as a rectangular parallelepiped of area A_p and variable height X_1 . The ground tube is defined to have the volume, V_t , below the bottom of the pillow, and the manometer of area A_m , is defined as existing above the plane of the bottom of the pillow.

The two quantities of interest are the equilibrium pillow height, X_1 and the height of fluid in the manometer, X_2 . Since two unknowns are to be determined, two equations are necessary. The appropriate equations are conservation of mass and equilibrium. Conservation of mass requires

$$m = \rho(T_p, \%) A_p X_1 + \rho(T_t, \%) V_t + \rho(T_m, \%) A_m X_2 \quad (1)$$

where:

A = area (m²)

m = total mass of methanol/water mixture (kg)

T = temperature (°C)

X_1 = height of top of pillow (m)

X_2 = height of fluid in manometer (m)

ρ = density, dependent on temperature T, and percent methanol, %, in the mix (kg/m^3),

and the subscripts are defined as follows:

m refers to manometer

p refers to pillow

t refers to ground tube.

It was determined that the density varies linearly with temperature to a very high degree of accuracy, so that the density curve is well represented as follows:

$$\rho(T, \%) = \rho_0(\%) - \beta(\%)T$$

where the density at 0°C , $\rho_0(\%)$, is only a function of percent methanol and the coefficient of cubical expansion, $\beta(\%)$, is also only a function of the mixture. Values of ρ_0 and β for 40, 50 and 60 percent mixes are given below. The procedure used to calculate the density curve is to interpolate between the percent methanol mixtures shown below. The ice point density and the coefficient of cubical expansion are thus obtained at the concentration of interest.

Density Curve Coefficients for Different Percent Mixes

Methanol Percent Mix	Ice Point Density, ρ_0 (kg/m^3)	Coefficient of Cubical Expansion, β ($\text{kg/m}^3 / ^\circ\text{C}$)
40	945.92	0.57314
50	928.66	0.66114
60	908.99	0.72343

The application of the principle of equilibrium leads to:

$$P_s + k(X_1 - X_0) - \rho(T_m, \%) gX_2 + \rho(T_p, \%) gX_1 = 0 \quad (2)$$

where:

g = acceleration of gravity (m/s^2)

k = pillow spring constant (N/m^3)

P_s = pressure on external pillow surface due to snow loading (N/m^2)

X_0 = empty, unloaded position of top of pillow (m),

and X_1 , X_2 , p , T_p , T and % are defined as before. X_2 may be eliminated from equation (1) by using equation (2). This yields:

$$X_1 = \frac{g[m - \rho(T_t, \%) V_t] / A_m + P_s - kX_0}{\rho(T_p, \%) g [1 + A/A_m] - k}$$

$$X_2 = \frac{[g\rho(T_p, \%) X_1 - P_s - k(X_1 - X_0)]}{\rho(T_m, \%) g}$$

In these equations, substitution of typical values indicates that the terms involving k are negligible compared to the other terms when P_s is not zero.

A computer program was written to evaluate these equations. The program was run using actual snow pillow summertime data for day 173 in 1979. Results are shown in Figure 7. In Figure 7, the small numerals 1, 2, 3 refer to the temperatures on top of, inside and underneath the pillow respectively. The small numeral 4 refers to the pressure transducer readings recorded and the circles refer to the predictions of the computer model. We note the strong correlation between the measured temperatures and the recorded pressure transducer readings. We also note that the computer analysis predicts only about one fourth of the variation in pressure observed.

The snow pillow inside temperature was used as the variable input to the program. During the day, field data indicates that the pillow temperature varied between 50°F and 111°F (10°C and 44°C). Based upon the measured pillow temperature variation, the computer model predicted a diurnal pressure change of 0.43 in. water in the system while the actual change was about 1.6 inches. The pressure change occurs as a result of the volume change of fluid within the pillow caused by the varying temperature. A pillow stiffness of 11.1 in. of H₂O/in. pillow deflection was assumed in the analysis. This value was selected to represent the measured skin stiffness values of 9.5 and 15.2 in. of H₂O/in. pillow deflection for the '78 and '79 California pillows respectively. In the analysis, the effect of doubling the skin stiffness is to double the pressure increase for a given increase in pillow temperature.

In the model, the predicted effect of varying the temperature of the tube connecting the pillow and manometer is negligible due to the small volume contained in the tube. Also, for a constant pillow pressure, the height of the methanol mixture in the manometer tube will vary as the density of the mixture within the manometer varies with temperature. For example, a 36°F (20°C) change in manometer tube temperature, holding all other variables constant, would yield a 1.5% variation in manometer reading for a 50% methanol solution. In this example, if the manometer was reading 25 inches at 32°F, and the tube temperature increased to 68°F later in the day while the pillow pressure remained constant, a new manometer reading of 25.36 inches would result. It should be noted that while this apparent change in pillow pressure would be recorded on the manometer, the pressure transducer would continue to read a constant pressure.

In summary, the current computer model can now account for only about 25% of the observed diurnal variation in pillow pressure. The larger variation observed can probably be explained by the presence of an air-water vapor - methanol vapor bubble within the pillow. A program has been written to analyze the effect of such a bubble. No results for the case with a bubble have been obtained yet.

6. Summary and Conclusions

The following conclusions were shown in the foregoing:

1. There is little or no effect on pillow/manometer system behavior due to varying tubing size and type.
2. Laboratory pillow response is not quite linear with peak deviations from linearity being about 2.0 in. H₂O.
3. The pillows appear to display about 0.6 in. H₂O of hysteresis.

4. The pillow skin stiffness is 9.5 to 15.2 in H₂O per inch of pillow skin deflection. The level of stiffness does not play an important role in predicting the slope of the pillow pressure vs. air pressure plot.
5. Pillows overweigh by up to 30 percent when subjected to loading by nonuniform stacks of bricks.
6. The theoretical model developed predicts only about 1/4 of the variation actually seen in summertime diurnal fluctuation. The model needs to have the effects of bubbles included to improve its predictive value.

7. Acknowledgments

The authors wish to gratefully acknowledge the financial and technical assistance of B. Shafer and A. Crook of the U.S.D.A. Soil Conservation Service. Jim Meiman has played an important coordination role in the conduct of this work. The work of John Wright, Pat Burns, Rick McClure, Jeff Hepler and Mark Havstad is also gratefully acknowledged.

TABLE I






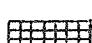

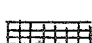




PILLOW LOADING CONFIGURATIONS			
TEST NAME	CODE LETTER	TOP VIEW	SIDE VIEW
PYRAMID	A		
WEDGE	B		
BLOCK	C		
DIAGONAL BLOCK	D		
DIAGONAL WEDGE	E		
HALF BLOCK	F		

TABLE II
NONUNIFORM LOADING EXPERIMENTS

Test Type	Test Description	Maximum Brick Height (No. of Bricks)	Measured Change in Pressure (in. H ₂ O)	Total Weight on Pillow (lbs)	H _{calc} 2880 in ² (in. H ₂ O)	H _{calc} 2592 in ² (in. H ₂ O)
C	1 flat layer	1	3.61	323.4	3.11	3.45
C	2 flat layers	2	7.07	646.8	6.22	6.91
C	3 flat layers	3	10.49	970.2	9.32	10.36
C	4 flat layers	4	13.84	1293.6	12.43	13.81
C	5 flat layers	5	17.27	1617	15.54	17.27
A	pyramid w/bricks	8	17.66	1617	15.54	17.27
A	interlocked	10	18.06	1617	15.54	17.27
A		12	18.31	1617	15.54	17.27
A		14	21.01	1617	15.54	17.27
A		16	22.35	1617	15.54	17.27
B	wedge	9	15.28	1617	15.54	17.27
B	wedge	11	13.66	1617	15.54	17.27
D	diagonal block	9	13.91	1617	15.54	17.27
E	diagonal block	12	12.18	1617	15.54	17.27
F	half block	10	15.86	1617	15.54	17.27
A	pyramid w/bricks	8	18.28	1617	15.54	17.27
A	not interlocked	10	18.82	1617	15.54	17.27
A		12	19.07	1617	15.54	17.27
A		14	20.26	1617	15.54	17.27
A		16	21.34	1617	15.54	17.27

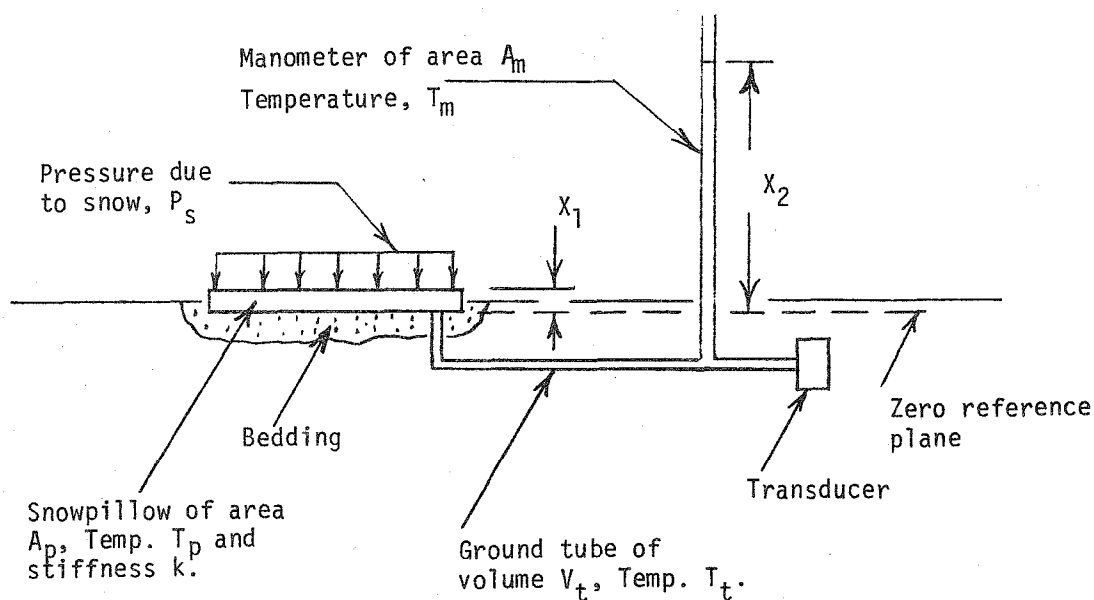


Figure 1. Snow Pillow, Manometer, Transducer System.

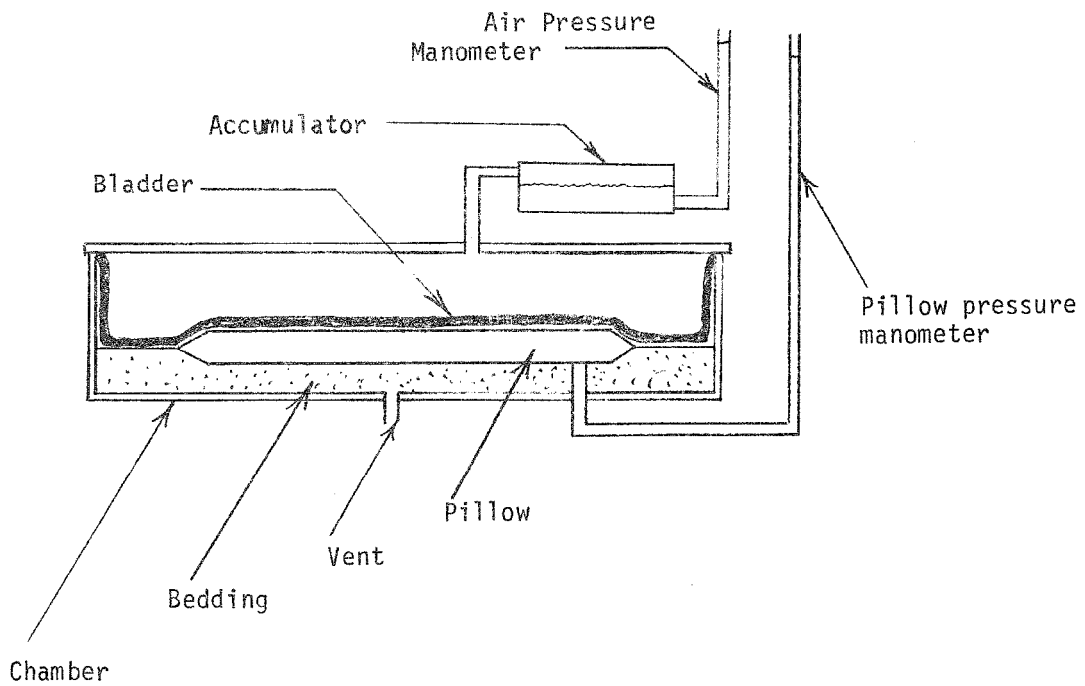


Figure 2. Pillow Test Chamber Apparatus

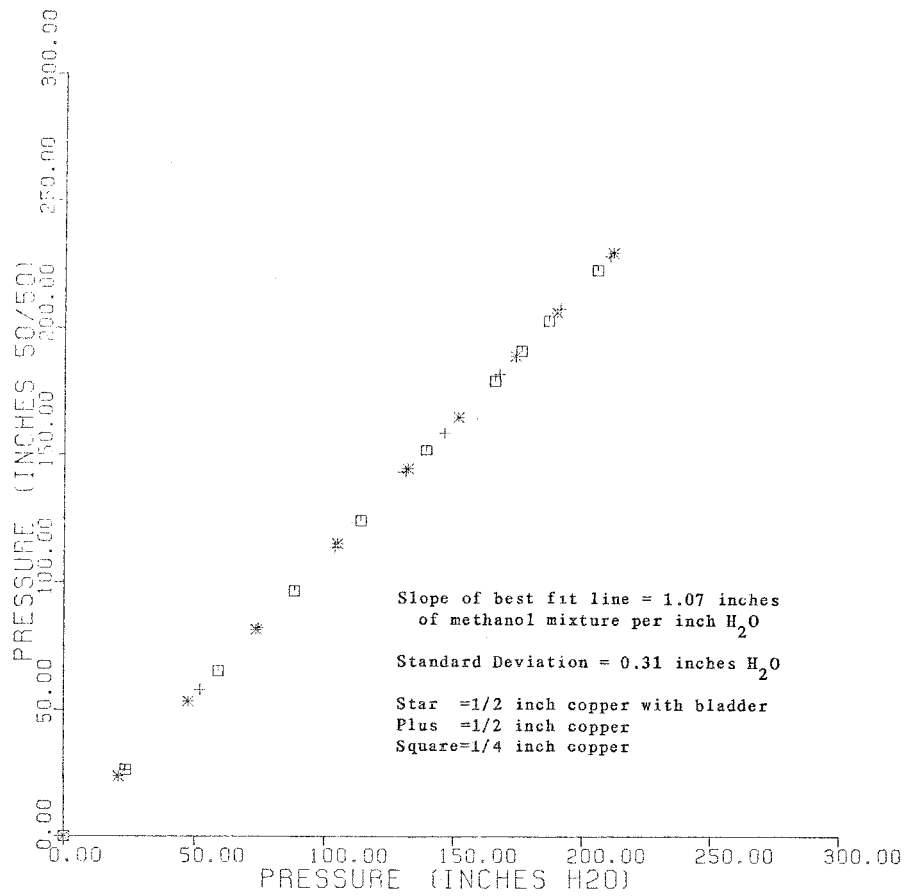


Figure 3. Pillow Response vs Applied Pressure for Various Tube Sizes

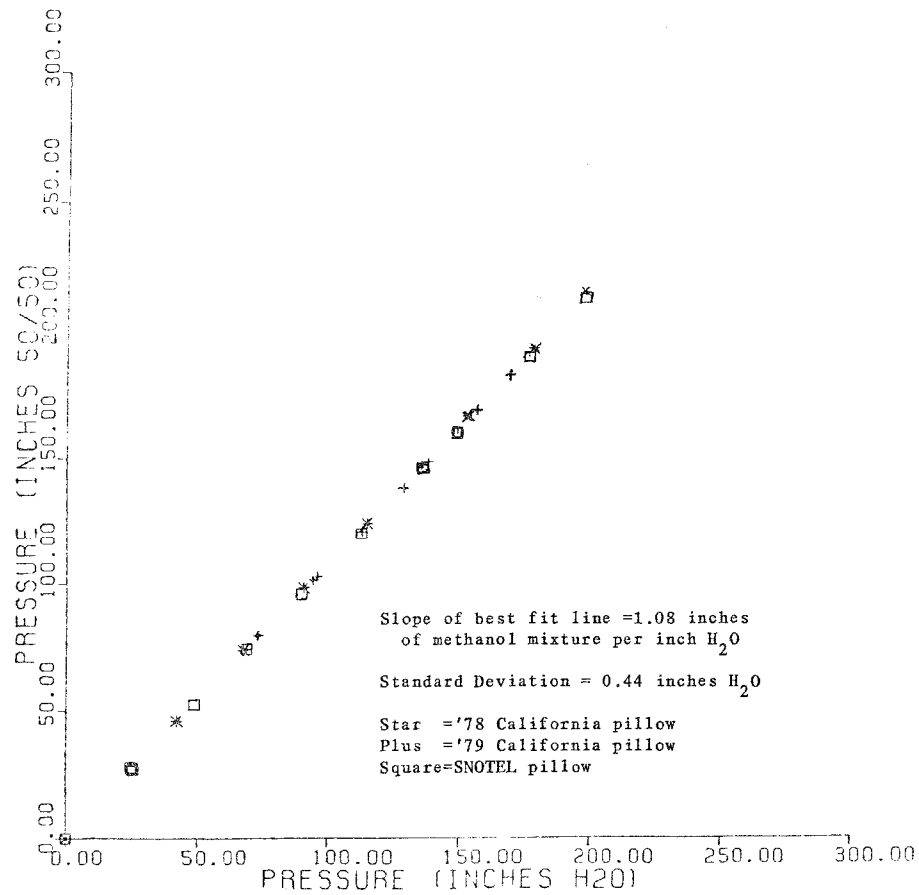


Figure 4. Laboratory Testing of Pillow Response vs Applied Pressure for Various Pillow Types

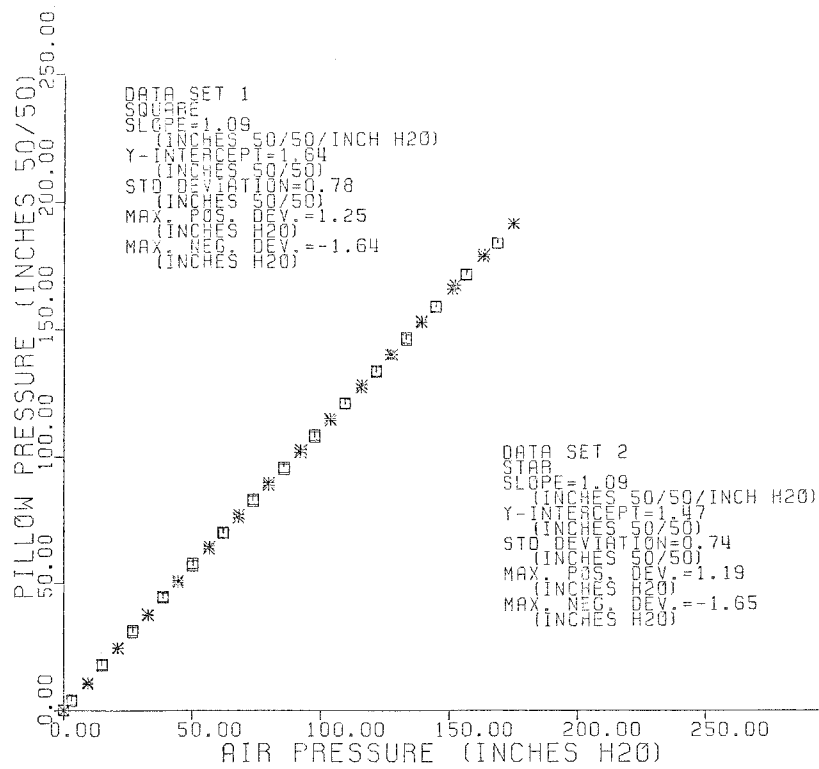


Figure 5. Pillow Response vs Applied Pressure

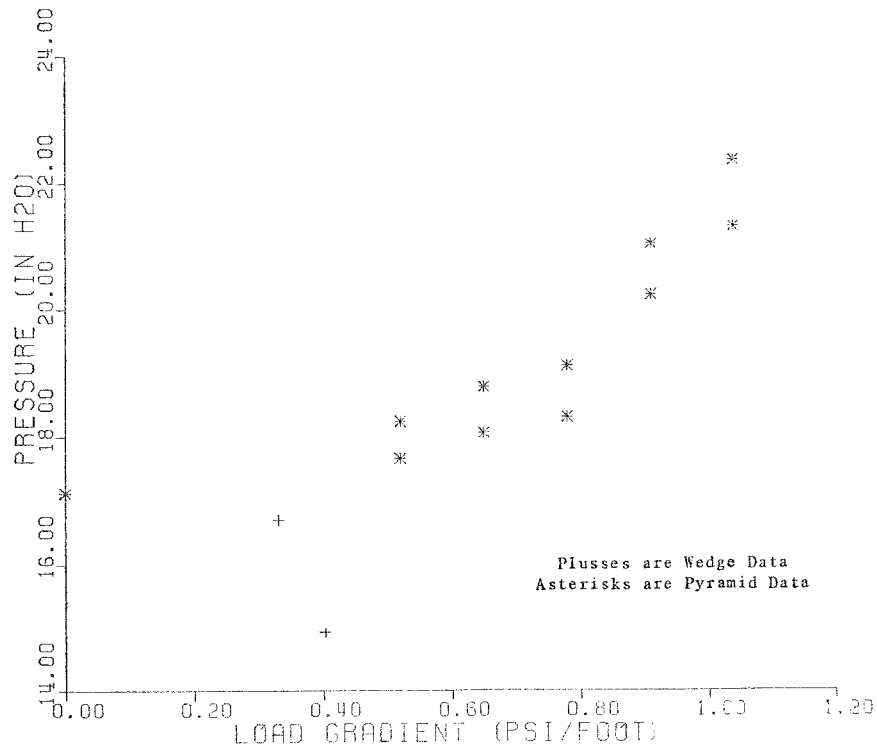


Figure 6. Measured pressure vs. load gradient for the brick tests with a constant 1617 lbs. of bricks.

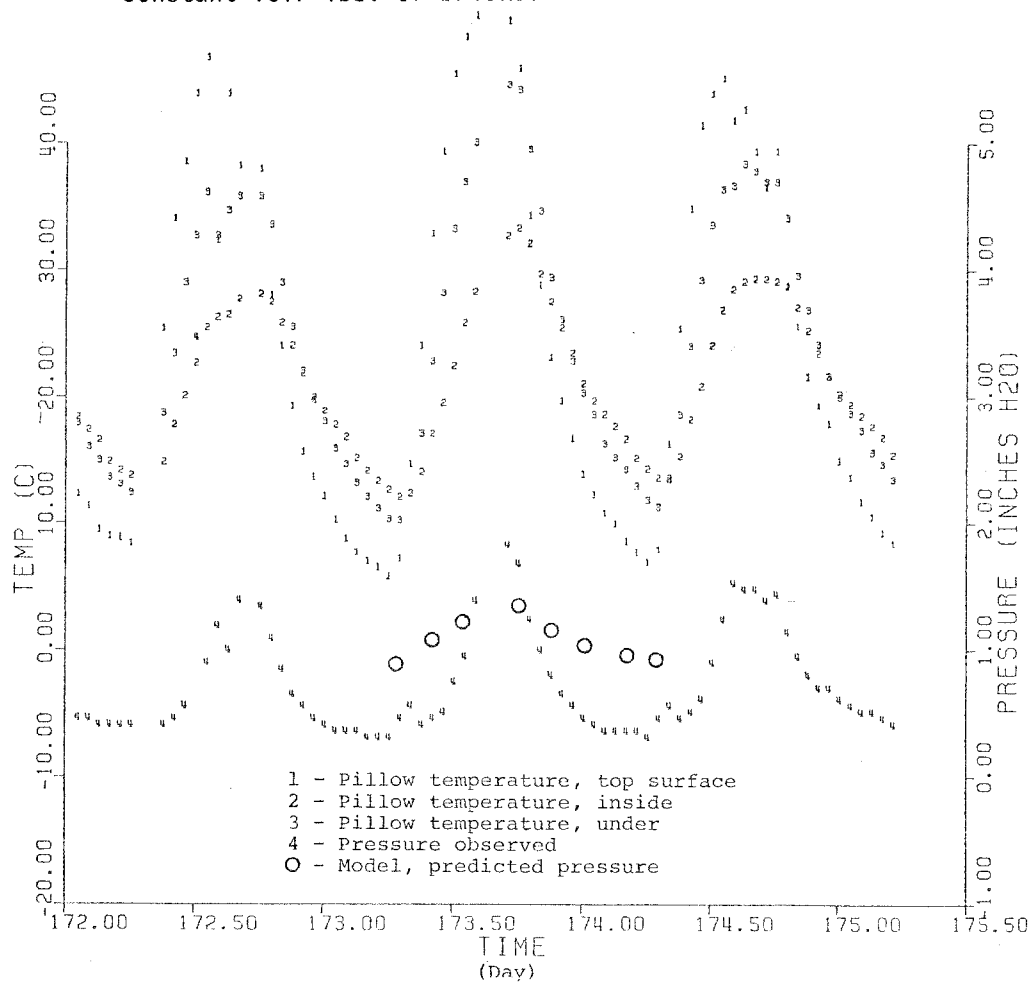


Figure 7. Pillow response to temperature.